Available online at www.sciencedirect.com
SCIENCE DIRECT®
ELSEVIER
Bioorganic & Medicinal Chemistry 12 (2004) 295–300
Bioorganic & Medicinal Chemistry

Saturation-transfer difference NMR studies for the epitope mapping of a carbohydrate-mimetic peptide recognized by an anti-carbohydrate antibody

Margaret A. Johnson and B. Mario Pinto*

Departments of Chemistry and of Molecular Biology and Biochemistry, Simon Fraser University, Burnaby, BC, Canada V5A 1S6

Received 16 May 2003; accepted 5 September 2003

Abstract—Saturation-transfer difference NMR spectroscopy (STD-NMR) experiments have been performed to analyze the topography or epitope of the octapeptide MDWNMHAA recognized by the anti-carbohydrate antibody SYA/J6 in solution; the antibody is directed against the *Shigella flexneri* Y *O*-antigen polysaccharide. The results permit a valuable comparison of solution versus crystal-structure data, and provide insight for the design of the next-generation binding ligands.

1. Introduction

Shigella flexneri Y is a Gram-negative enterobacterium that causes bacillary dysentery by invading the colonic mucosa.[1] The O-antigen polysaccharide forms part of the cell-surface lipopolysaccharide, which is antigenic and therefore provides a suitable vaccine candidate. The O-polysaccharide consists of the repeating unit →2)-α-L-Rha-(1→2)-α-L-Rha-(1→3)-α-L-Rha-(1→3)-β-D-GlcNAc-(1→ (**1**) (Scheme 1).[2,3] However, the development of vaccines based on polysaccharides may be complicated by several factors, including poor immunogenicity, and poor response in infants.[4] In several cases, these factors have been circumvented, with considerable success, by conjugation of polysaccharides to proteins.[4] An alternative strategy is the use of carbohydrate-mimetic peptides, which have demonstrated immunogenic potential.[5] Peptide ligands have been identified for a wide range of anti-carbohydrate antibodies, and for a limited number of other carbohydrate-binding proteins.[5] These peptides are specific molecular mimics of carbohydrates, and in general, bind with similar or greater affinity to receptors.[5] Significantly, immunological studies showed that in some cases, these peptides could not only bind to anti-carbohydrate antibodies, but could induce an immune response against the original carbohydrate.[5]

An understanding of peptide-carbohydrate mimicry requires detailed knowledge of the topography of the ligands of both classes recognized by complementary protein receptors. Analysis of the topography, or epitope mapping, may be performed by a variety of methods.[6] The use of NMR spectroscopy permits a direct characterization of protein–ligand interactions at the molecular level. Thus, a combination of transferred NOE (trNOE)[7] and saturation-transfer difference (STD)[8–11] experiments has been used to probe the conformations of ligands bound to receptors and to define the critical epitope, that is, the portions of the ligand in close contact with the protein.[12] These data are useful in the construction and validation of models of protein-ligand complexes.[13] In addition, binding ligands have been identified from complex mixtures of compounds by STD-NMR experiments.[9] Vogtherr and Peters[14] have described the use of STD-NMR spectroscopy, in combination with chemical modification, for the simultaneous epitope mapping of a library of ligands, and the use of STD-2D-NMR methods, for example, STD-TOCSY and STD-HMQC. We have recently described a STD-1D-TOCSY sequence for more rapid epitope mapping.[13]

As part of our program to study the nature and origin of peptide-carbohydrate mimicry and to develop peptide-based vaccines, the crystal structures of complexes of the anti-carbohydrate monoclonal antibody (mAb)

Keywords: peptide-carbohydrate mimicry; saturation-transfer difference NMR; peptide epitope mapping; molecular recognition in solution vs. solid state.
Abbreviations: MAb-monoclonal antibody; Fab-antigen binding fragment; STD-saturation-transfer difference.
* Corresponding author. Tel.: +1-604-291-4327; fax: +1-604-291-5424; e-mail: bpinto@sfu.ca

0968-0896/$ - see front matter © 2003 Elsevier Ltd. All rights reserved.
doi:10.1016/j.bmc.2003.09.041

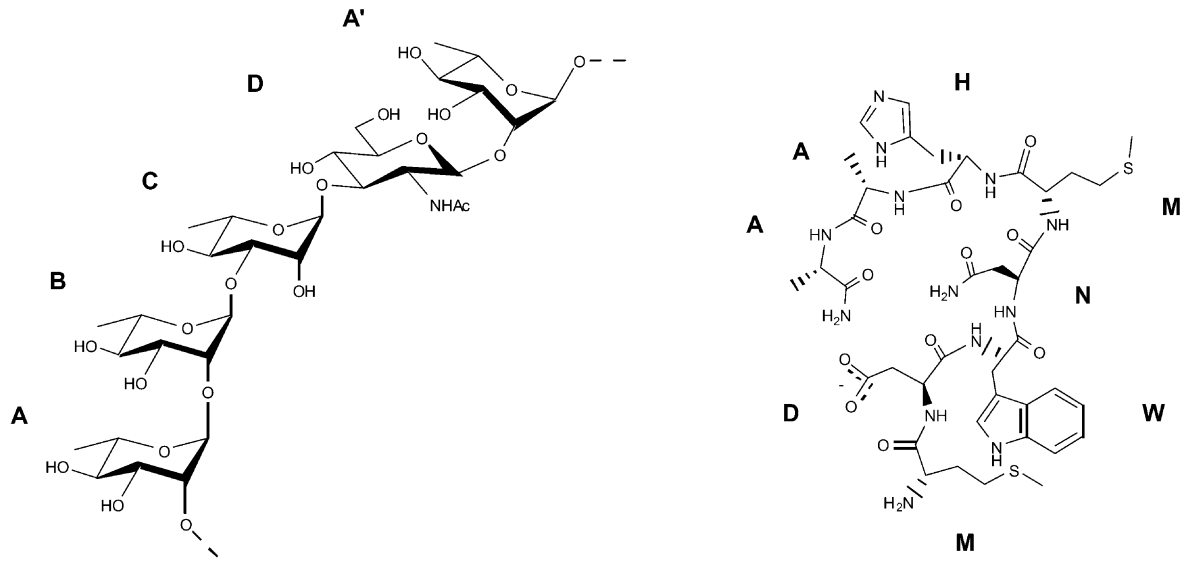

1 2

Scheme 1. The lipopolysaccharide O-antigen of *Shigella flexneri* Y (**1**) and an octapeptide molecular mimic, MDWNMHAA (**2**).

SYA/J6 with carbohydrate[15,16] and mimetic peptide, MDWNMHAA **2**[17] ligands (Scheme 1) were determined, revealing the nature of mimicry in this system. The peptide proved to be a partial structural mimic of the carbohydrate, providing several similar interactions with the combining site, but also taking advantage of areas of the site not contacted by the carbohydrate. Interestingly, water molecules were extensively involved in binding, bridging between the peptide and antibody through hydrogen bonding.[17] It is of interest to study the same system using solution NMR techniques in order to identify similarities and differences in molecular recognition, and to investigate the potential of these complementary methods. Such knowledge will be useful (1) to probe the validity of information obtained in the solid state, (2) to provide a complementary, faster method of analysis, and (3) to assist in the design of the next-generation binding ligands. We report here a study of the peptide-antibody complex by STD-NMR spectroscopy,[8–11] and demonstrate the potential of solution NMR techniques for epitope mapping and the study of protein–ligand interactions.

2. Results and discussion

The 1D STD-NMR spectrum of the octapeptide **2** in the presence of the antigen binding fragment (Fab) of the mAb SYA/J6 is shown in Figure 1. Saturation produced strong enhancements of the Trp-3 ring protons and the Met-5 side-chain protons. In addition, both Met-1 and Met-5 methyl groups were enhanced, with one enhanced more strongly than the other.

The crystal structure of the Fab-MDWNMHAA **2** complex[17] reveals that the side chain of Met-5 is in close contact with the Trp H33 indole ring, consistent with the strong enhancements. In contrast, Met-1 is largely exposed to solvent; only its ε-methyl group makes a few contacts with the antibody. On this basis, the more strongly enhanced ε-methyl signal (2.08 ppm) was attributed to Met-5, while the more weakly enhanced ε-methyl signal (1.96 ppm) is likely that of Met-1. One of each of the γ-methylene protons of Met-1 and Met-5 are enhanced (Fig. 2, Table 1), and in addition, the overlapping resonance of the other methylene protons, at 2.4 ppm, is enhanced. The latter enhancement likely has a contribution from Met-5, as both of its γ-methylene protons are in close contact with Trp H33 (Fig. 3). The enhancement of the Met-1 γ-methylene proton at 2.3 ppm, however, is difficult to explain, as it is not within 5 Å of any antibody proton in the crystal structure. The Met-1 α-proton is not enhanced, consistent with the crystal structure in which the N-terminus of the peptide is far from the antibody surface. We conclude that the terminus of the Met-1 side chain in the bound solution conformation does contact the antibody, unlike that in the crystal structure.

Strong enhancements of all the Trp-3 ring protons were observed (Figs 1 and 3, Table 1). This is also consistent with the crystal structure, which shows that Trp-3 is buried in a hydrophobic pocket composed of residues from CDR L3 (Thr L91, Val L94, Pro L95) and a framework residue (Trp H47). The contacts with the pocket are extensive. Even an enhancement of the Hε1 proton (10.13 ppm) is observed.

Enhancements of both Ala β-methyl groups were observed (Figs 1 and 2). This is consistent with the crystal structure, which shows that the Ala-7 methyl group makes contact with Tyr L32, at the top of another hydrophobic pocket in the binding site, while the Ala-8 methyl group contacts the Trp H33 side chain,

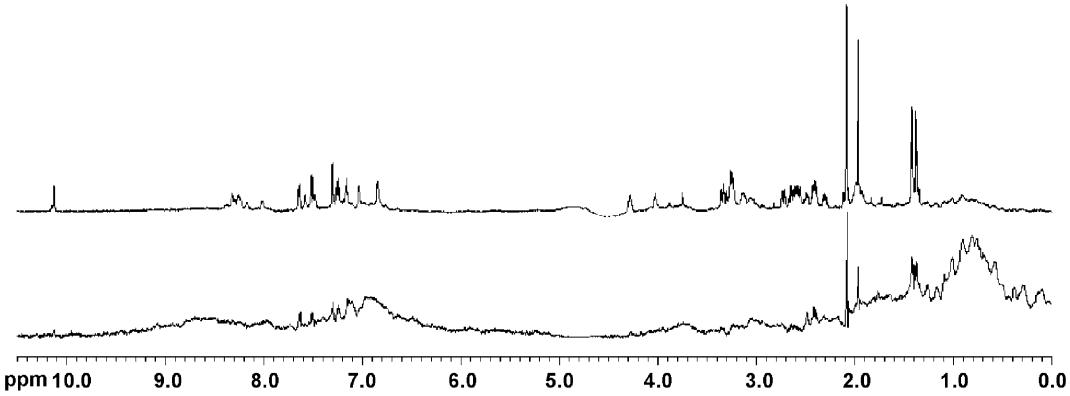

Figure 1. 1D ^{1}H NMR spectrum (top) and 1D STD-NMR spectrum (bottom) of the octapeptide **2** in the presence of the antibody. Intensities are given in Table 1.

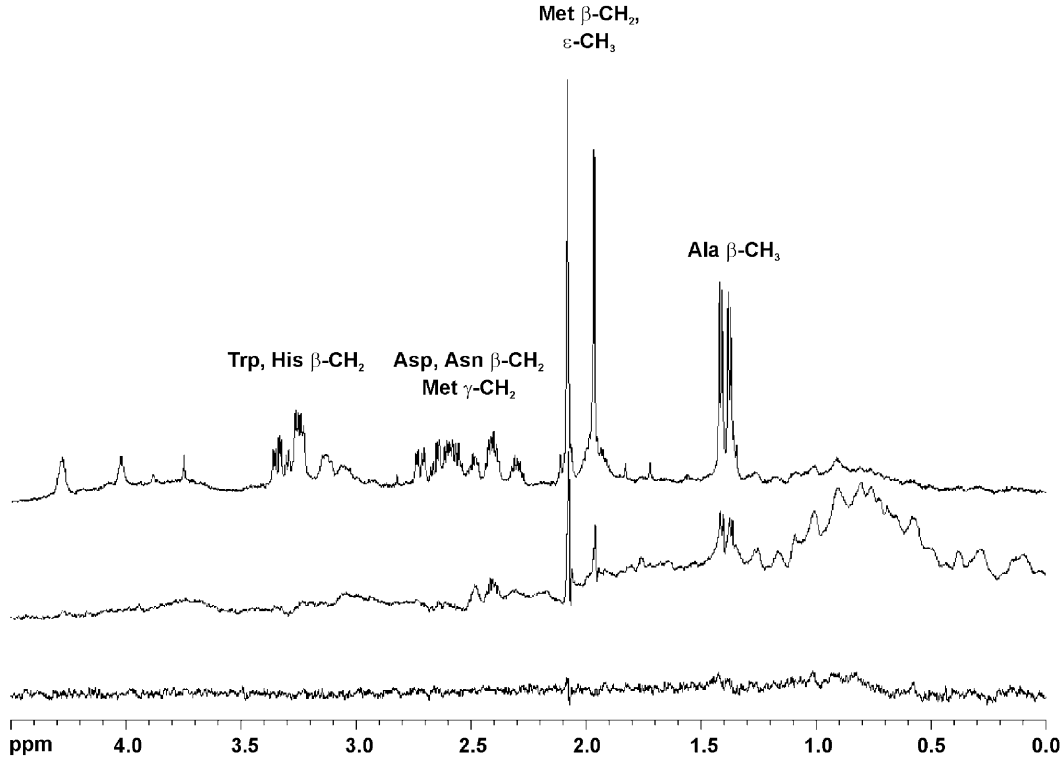

Figure 2. Expansions of the 1D ^{1}H NMR spectrum (top), 1D STD-NMR spectrum (middle), and 1D STD-NMR spectrum with spin-lock pulse (bottom) of the octapeptide **2** in the presence of the antibody. Intensities are given in Table 1.

adding to the hydrophobic contacts made by Met-5.

Other enhancements consistent with the crystal structure are those of Asp-2 and Asn-4. The β-CH_2 hydrogens of Asp-2 are minimally enhanced, while those of Asn-4 show stronger enhancements, consistent with more extensive contact with the binding site (Figs 1 and 2, Table 1).

Interestingly, few enhancements were observed for the amide hydrogens of the peptide. These hydrogens make few direct contacts with the binding site. Rather, the amide hydrogens of Trp-3, Asn-4, and Met-5 all form hydrogen bonds to water molecules, which act as hydrogen-bonded bridges between the peptide and antibody. Only the Trp-3 amide hydrogen, with five other neighboring hydrogens (<5 Å) in the binding site, shows an enhancement. Evidently, the present STD-NMR experiment either does not detect contacts mediated through water molecules or alternatively, these bound water molecules are not present in the complex in solution. The amide hydrogens of His-6, Ala-7 and Ala-8 are all involved in intramolecular hydrogen bonds with Asn-4, which stabilize the α-helical turn conformation of the last four residues of the peptide. However, the amide hydrogens of His-6 and Met-5 are in close proximity to five and eight neighboring hydrogens, respectively, yet do not show enhancements. This observation points to a difference between the bound ligand conformation in solution and in the solid state.

Another point of difference between the crystallographic and STD-NMR spectroscopic data is in the contact of His-6. The STD-NMR data indicate that the β-CH_2

Table 1. Enhancements observed in the STD-NMR spectrum of the octapeptide **2** in the presence of the Fab, and distances to atoms within the antibody combining site[a]

Resonance	δ (ppm)	STD enhancement[b] (%)	Closest distance to antibody (heavy atoms)	# Nearby antibody hydrogens (<5 Å)
Ala-7Hβ	1.38	39	3.73	8
Ala-8Hβ	1.41	44	3.46	5
Met-1/5Hβ	*1.98–2.01*	*43*	*5.57 (Met-1), 3.6 (Met-5)*	*8 (Met-5Hβ2), 0 (Met-1Hβ1)*
Met-1/5Hβ	*1.93–1.95*	*0*	*5.57 (Met-1), 3.6 (Met-5)*	*0 (Met-1Hβ2), 2 (Met-5Hβ1)*
Met Hε	*1.97*	*34*	*if 1: 3.78*	*2*
Met Hε	*2.08*	*67*	*if 5: 3.48*	*16*
Met-1Hγ	*2.3*	*56*	5.09	0 (Met-1Hγ)
Met-1/5Hγ	*2.40*	*72*	*5.09 (Met-1), 3.56 (Met-5)*	*0 (Met-1Hγ), 10 (Met-5Hγ2)*
Met-5Hγ	*2.48*	*100*	*3.56*	*13 (Met-5Hγ1)*
Asp-2/Asn-4Hβ	*2.58*	*32*	*4.54 (Asp-2), 4.02 (Asn-4)*	*2 (Asp-2Hβ2), 9 (Asn-4Hβ2)*
Asn-4Hβ	*2.65*	*42*	*4.02*	*12 (Asn-4Hβ1)*
Asp-2Hβ	*2.71*	*0*	*4.54*	*1 (Asp-2Hβ1)*
His-6Hβ	*3.13*	*0*	*3.43*	*8 (His-6Hβ1)*
His-6/Trp-3Hβ	*3.25*	*0*	*3.43 (His-6), 3.59 (Trp-3)*	*9 (His-6Hβ2), 10 (Trp-3Hβ1)*
Trp-3Hβ	*3.34*	*13*	3.59	*11 (Trp-3Hβ2)*
Met-1Hα	4.02	0	6.59	0
Ala-8, Met-5, Ala-7Hα	4.27–4.29	23	4.89 (Ala-8), 4.18 (Met-5), 3.52 (Ala-7)	2 (Ala-8), 3 (Met-5), 5 (Ala-7)
C-terminal $CONH_2$	6.85	0		
Asn Hδ2	7.03	0	3.03	*15 (Asn-4Hδ21)*
Trp-3Hζ3	7.15	88	3.70	13
Trp-3Hη2	7.25	54		11
Trp-3Hδ1 (His-6Hδ2)	7.30	42	3.37	9
Asn-4Hδ2	7.48	0	3.03	*11 (Asn-4Hδ22)*
Trp-3Hζ2	7.51	49	3.59	7
C-terminal $CONH_2$	7.58	0		
Trp-3Hε3	7.64	65	3.76	13
Met-5HN	8.01	0	3.80	8
Ala-7HN	8.17	0	3.51	3
Ala-8HN	8.22	0	5.30	2
Asn-4HN	8.26	0	3.32	3
His-6HN	8.29	0	4.08	5
Trp-3HN	8.32	21	4.20	5
Trp-3Hε1	10.13	25	3.58	7

[a] Rows corresponding to resonances that are not stereospecifically or regiospecifically assigned are shown in italics.
[b] Normalized to the strongest enhancement, Met-5Hγ (2.48 ppm).

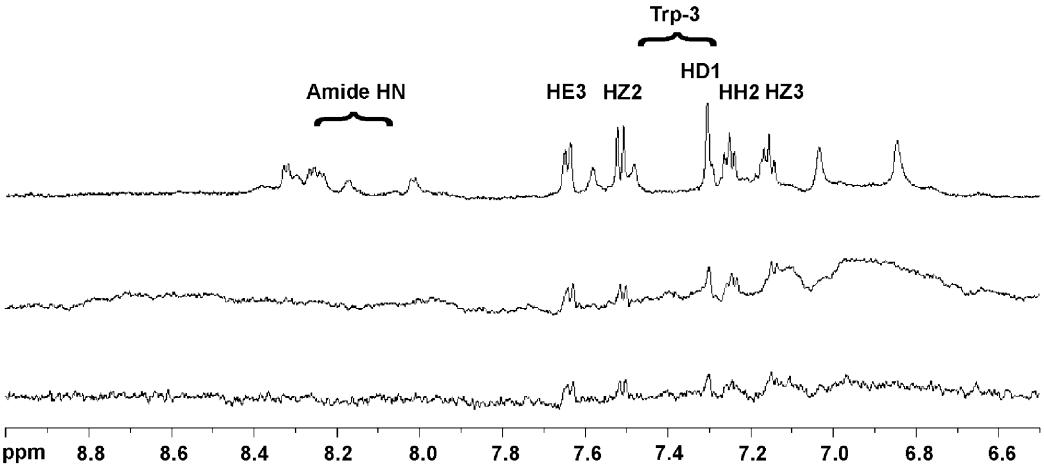

Figure 3. Expansions of the amide HN and aromatic region of the 1D ^{1}H NMR spectrum (top), 1D STD-NMR spectrum (middle), and 1D STD-NMR spectrum with spin-lock pulse (bottom) of the octapeptide **2** in the presence of the antibody. Intensities are given in Table 1.

methylene hydrogens of His-6 are not enhanced, although they are close to many antibody hydrogens in the crystal structure. It is possible that since this residue is located on the surface of the binding groove, its side chain may adopt a more exposed position in solution, with the His-6 side chain forming only one hydrogen bond to Tyr L32 OH. However, even in this conformation, the His-6 β-CH_2 methylene hydrogens are still within 5 Å of many hydrogens in the antibody combining site.

The other side-chain protons of this residue could not be observed, probably due to rapid exchange. Interestingly, only one of the Trp-3 β-CH_2 protons was enhanced, although both are close to the antibody (Table 1).

A significant point of difference with the crystallographic data is observed with the contact to the Asn-4 residue. Here, no enhancement was observed for the

Asn-4Hδ side chain hydrogens. This is surprising since this side-chain is located deep within the binding site, where one amide hydrogen forms a hydrogen bond to Thr L91 O, while the other acts as a hydrogen bond donor to Ala-7 O. Both hydrogens have many near neighbors in the binding site and enhancements would be expected. An alternative binding mode with rotation of the Asn-4 side chain to bind to water molecules within the deepest part of the site is possible; however, this would require loss of the four intramolecular hydrogen bonds provided by the Asn-4 side chain, and therefore, this explanation is not considered likely.

Strong enhancements of the hydrogens on the Fab were also observed, and experiments employing a spin-lock pulse to reduce the intensities of these resonances were performed. A similar pattern of enhancements was observed; however, the ligand resonances were also significantly reduced (Figs 2 and 3, bottom spectra), so that little additional information could be obtained. However, a small enhancement of one of the Asn-4 side chain amide hydrogens (Fig. 3, bottom spectrum; 7.03 ppm) was observed.

Transferred NOE effects for the peptide–antibody complex were not observed. This is likely due to unfavorable binding kinetics; if the off-rate for the complex is not significantly greater than the NOE buildup rate in the complex, efficient transfer of the NOEs representative of the bound conformation to the free state of the ligand will not occur.[7] However, the saturation times employed in the STD-NMR experiment are longer than the mixing times employed in transferred NOE experiments (typical values, and those employed in this study, are 2 s and $\leq$300 ms, respectively) and this extra time for NOE buildup may allow the observation of STD-NMR effects even when trNOEs are not observable.

The observed STD-NMR enhancements were mapped onto the crystal structure of the peptide–antibody complex, and define a molecular surface that generally correlates well with the epitope surface observed in the crystal structure, although with a few differences (Fig. 4). These differences help to reveal parts of the ligand that are more mobile or more exposed to solvent within the complex. Thus, the structural features of the complex are not exactly the same in solution and in the solid state.

The knowledge gained from the STD-NMR work will guide further development for increasing peptide affinity through modifications in order to minimize or eliminate the competing, deleterious effect of the exposure of the N- and C-termini of the octapeptide with water molecules. A rapid, functional assessment of critical residues by mutational analysis of the parent peptide, for example by synthesis on pins,[18] combined with STD-NMR spectroscopic analysis may, therefore, be an efficient method for the design of the next-generation binding ligands. Furthermore, the STD-NMR data indicate that the N-terminus of Met-1, since it does not contact the antibody surface, could likely be used to link the MDWNMHAA peptide to protein carriers to generate vaccines without significant deleterious effects. Finally, transferred NOE data, in conjunction with STD data, could be used to design higher affinity ligands, for example, by enhancing helicity in the C-terminus. Increasing the affinity of a hapten for its complementary antibody in this way could lead to an enhanced immune response, as demonstrated recently for the case of the immune response to constrained nicotine conformations.[19]

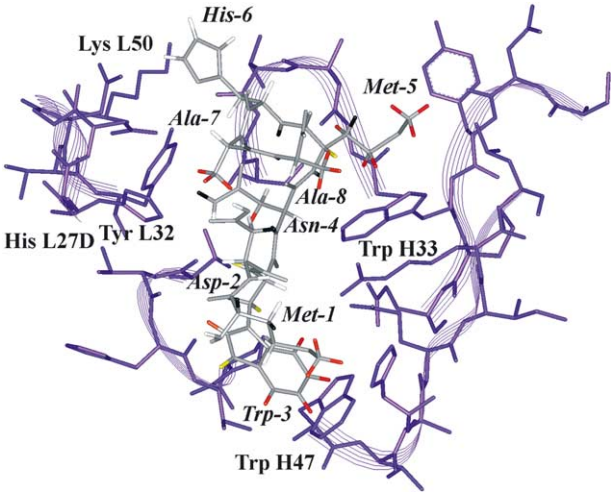

Figure 4. The crystal structure of the antibody–(**2**) complex, with STD-NMR intensities mapped onto the bound peptide. Residues of the antibody combining site are shown in purple, with selected residues labeled, and the direction of the backbone indicated in ribbon representation. Residues of the peptide are labeled in italics. Heavy atoms of the peptide are shown in gray, while the default color for hydrogen atoms is white. Observed STD-NMR intensities are mapped onto hydrogen atoms of the peptide by color, with red indicating 50–100% enhancement, orange 30–50% enhancement, and yellow <30% enhancement. Protons that are definitely *not* enhanced are shown in black; those for which no enhancement could be determined (due to interference by other resonances, or not observable in the 1D spectrum) remain white.

3. Methods

3.1. NMR spectroscopy

The octapeptide, MDWNMHAA **2**, was purchased from the Alberta Peptide Institute. NMR spectra were recorded on a Bruker AMX-600 NMR spectrometer. Chemical shifts were referred to external 3-(trimethylsilyl)-1-propanesulfonic acid (DSS). An NMR sample of the mAb SYA/J6 Fab fragment[16] (0.14 mM) was prepared in phosphate-buffered saline solution (12 mM K_2HPO_4/KH_2PO_4, 137 mM NaCl, 3 mM KCl, 0.02% NaN_3, 10% D_2O, pH 6.1) and octapeptide **2** (1.69 mg, 1.73 μmol) was added to the sample, for a final peptide concentration of 2.9 mM and a ratio of 20:1 **2**:antibody. Resonances of **2** were assigned using 2D-TOCSY and ROESY NMR spectroscopy. No trNOE effects were observed. All 1D NMR spectra were recorded with 64 scans and 32 K data points, and processed by zero-filling to 64 K points and multiplication by an exponential function, followed by Fourier transformation. Data processing was performed using XWINNMR (Bruker) software. 1D STD-NMR spectra were recorded at 298 K with 1024 scans, with selective saturation of protein

resonances at 0 ppm (30 ppm for reference spectra) using a series of 40 Gaussian shaped pulses (50 ms, 1 ms delay between pulses, $\gamma B_1/2\pi = 110$ Hz), for a total saturation time of 2.04 s. For certain experiments, a 10 ms spin-lock pulse ($\gamma B_1/2\pi = 11$ kHz) was applied after excitation to reduce the intensity of broad protein resonances. Subtraction of saturated spectra from reference spectra was performed by phase cycling.[8,9] Measurement of enhancement intensities was performed by direct comparison of STD-NMR spectra and reference 1D spectra.

3.2. Molecular modeling

Molecular modeling and visualization were performed using InsightII/Discover software (Accelrys, Inc.) implemented on a Silicon Graphics O2 platform.

Acknowledgements

We are grateful to D. R. Bundle for providing the monoclonal antibody SYA/J6, and to F. A. Quiocho and N. K. Vyas for providing X-ray structural coordinates of the SYA/J6 Fab and its complexes prior to publication. This work was supported by the Natural Sciences and Engineering Research Council of Canada (including a postgraduate scholarship to M. A. J.).

References and notes

1. Hale, T. L. In *Topley and Wilson's Microbiology and Microbial Infections*, Hansler, W. J., Shuman, M., Eds.; Arnold: London, 1998, Vol. 3, p 479.
2. Kenne, L.; Lindberg, B.; Petersson, K.; Romanowska, E. *Carbohydr. Res.* **1977**, *56*, 363. Kenne, L.; Lindberg, B.; Petersson, K.; Katzenellenbogen, E.; Romanowska, E. *Eur. J. Biochem.* **1977**, *76*, 327. Kenne, L.; Lindberg, B.; Petersson, K.; Katzenellenbogen, E.; Romanowska, E. *Eur. J. Biochem.* **1978**, *91*, 279.
3. Bundle, D. R.; Gidney, M. A. J.; Josephson, S.; Wessel, H.-P. Synthesis of *Shigella flexneri* O-Antigenic Repeating Units. Conformational Probes and Aids to Monoclonal Antibody Production. In *ACS Symp. Ser.*; Anderson, L., Unger, F. M., Eds.; American Chemical Society: Washington, 1983; Vol. 231, p 49. Carlin, N. I. A.; Gidney, M. A. J.; Lindberg, A. A.; Bundle, D. R. *J. Immunol.* **1986**, *137*, 2361.
4. Lindberg, A. A. *Vaccine* **1999**, *17* (Suppl. 2), S28. Robbins, J. B.; Schneerson, R.; Szu, S. C.; Pozsgay, V. *Pure Appl. Chem.* **1999**, *71*, 745. Jennings, H. J. *Curr. Top. Microbiol. Immunol. C* **1990**, *125*, 373. Jennings, H. J. *Adv. Exp. Med. Biol.* **1988**, *228*, 495. Lee, C. J. *Mol. Immunol.* **1987**, *24*, 1005. Jennings, H. J. *Adv. Carbohydr. Chem. Biochem.* **1983**, *41*, 155.
5. Johnson, M. A.; Pinto, B. M. *Aust. J. Chem.* **2002**, *55*, 13, and references cited therein.
6. Morris, G. E. In *Biomolecular Methods Handbook*; Rapley, R., Walker, J. M., Eds.; Totowa: Humana, 1998; p 619.
7. Clore, G. M.; Gronenborn, A. M. *J. Magn. Reson.* **1983**, *53*, 423. Clore, G. M.; Gronenborn, A. M. *J. Magn. Reson.* **1982**, *48*, 402. Albrand, J. P.; Birdsall, B.; Feeney, J.; Roberts, G. C. K.; Burgen, A. S. V. *Int. J. Biol. Macromol.* **1979**, *1*, 37. Balaram, P.; Bothner-By, A. A.; Dadok, J. *J. Am. Chem. Soc.* **1972**, *94*, 4015. Balaram, P.; Bothner-By, A. A.; Breslow, E. *J. Am. Chem. Soc.* **1972**, *94*, 4017.
8. Mayer, M.; Meyer, B. *Angew. Chem. Int. Ed.* **1999**, *38*, 1784.
9. Klein, J.; Meinecke, R.; Mayer, M.; Meyer, B. *J. Am. Chem. Soc.* **1999**, *121*, 5336.
10. Peters, T.; Meyer, B. Ger. Patent No. DE19649359; Swiss Patent No. 690695; UK Patent No. GB23211401; US Patent pending.
11. Mayer, M.; Meyer, B. *J. Am. Chem. Soc.* **2001**, *123*, 6108.
12. Möller, H.; Serttas, N.; Paulsen, H.; Burchell, J. M.; Taylor-Papadimitriou, J.; Meyer, B. *Eur. J. Biochem.* **2002**, *269*, 1444. Kooistra, O.; Herfurth, L.; Lüneberg, E.; Frosch, M.; Peters, T.; Zähringer, U. *Eur. J. Biochem.* **2002**, *269*, 573. Haselhorst, T.; Weimar, T.; Peters, T. *J. Am. Chem. Soc.* **2001**, *123*, 10705. Meinecke, R.; Meyer, B. *J. Med. Chem.* **2001**, *44*, 3059. Weimar, T.; Bukowski, R.; Young, N. M. *J. Biol. Chem.* **2000**, *275*, 37006. Maaheimo, H.; Kosma, P.; Brade, L.; Brade, H.; Peters, T. *Biochemistry* **2000**, *39*, 12778.
13. Johnson, M. A.; Pinto, B. M. *J. Am. Chem. Soc.* **2002**, *124*, 15368.
14. Vogtherr, M.; Peters, T. *J. Am. Chem. Soc.* **2000**, *122*, 6093.
15. Vyas, M. N.; Vyas, N. K.; Meikle, P. J.; Sinnott, B.; Pinto, B. M.; Bundle, D. R.; Quiocho, F. A. *J. Mol. Biol.* **1993**, *231*, 133.
16. Vyas, N. K.; Vyas, M. N.; Chervenak, M. C.; Johnson, M. A.; Pinto, B. M.; Bundle, D. R.; Quiocho, F. A. *Biochemistry* **2002**, *41*, 13575.
17. Pinto, B. M.; Scott, J. K.; Harris, S. L.; Johnson, M. A.; Bundle, D. R.; Chervenak, M. C.; Vyas, M. N.; Vyas, N. K.; Quiocho, F. A. 1998, XIX International Carbohydrate Symposium, San Diego, USA; Abstr. CP 132, CO 019. Vyas, N. K.; Vyas, M. N.; Chervenak, M.C.; Bundle, D. R.; Pinto, B. M.; Quiocho, F. A., *Proc. Natl. Acad. Sci.* USA, in press.
18. Multipin™ peptide synthesis kit manual (MacIntosh version), Chiron Mimotopes, Clayton, Australia, 1989. Geysen, H. M.; Meloen, R. H.; Barteling, S. J. *Proc. Nat. Acad. Sci. U.S.A* **1984**, *81*, 3998. Geysen, H. M.; Rodda, S. J.; Mason, T. J.; Tribbick, G.; Schoofs, P. G. *J. Immunol. Meth.* **1987**, *102*, 259. Geysen, H. M.; Tainer, J. A.; Rodda, S. J.; Mason, T. J.; Alexander, H.; Getzoff, E. D.; Lerner, R. A. *Science* **1987**, *235*, 1184. Getzoff, E. D.; Geysen, H. M.; Rodda, S. J.; Alexander, H.; Tainer, J. A.; Lerner, R. A. *Science* **1987**, *235*, 1191.
19. Meijler, M. M.; Matsushita, M.; Altobell, L. J., III; Wirsching, P.; Janda, K. D. *J. Am. Chem. Soc.* **2003**, *125*, 7164.